Metrol. Meas. Syst., Vol. 31 (2024) No. 1, pp. 153–164
DOI: 10.24425/mms.2023.148545

PAN POLSKA AKADEMIA NAUK

METROLOGY AND MEASUREMENT SYSTEMS
Index 330930, ISSN 0860-8229
www.metrology.wat.edu.pl

M&MS

THE INFLUENCE OF TEMPERATURE ON SPECTRAL CHARACTERISTICS OF SILICON PHOTOVOLTAIC CELLS

Jacek Dąbrowski, Łukasz Buchert, Janusz Zarębski

Gdynia Maritime University, Faculty of Electrical Engineering, Department of Marine Electronics, ul. Morska 81-87, 81-225 Gdynia, Poland (✉ *j.dabrowski@we.umg.edu.pl*)

Abstract

The paper presents the results of research on commercial photovoltaic cells made of crystalline silicon. In particular, the focus was on the description of the elaborated by the authors measuring system with measurements methodology used for assessment of the influence of temperature on spectral characteristics of the tested cells, describing the dependence of the current sensitivity (spectral response, responsivity) and the external quantum efficiency on the wavelength of optical radiation. The investigations carried out in the proposed test system made it possible to evaluate the properties of the cells in the conditions similar to the operating conditions.

Keywords: photovoltaic cell, spectral response, external quantum efficiency, optical radiation.

1. Introduction

Photovoltaics is one of the most intensively developing fields in both science and technology. Currently, the most popular and most frequently used solar cells (PV cells) in photovoltaic circuits and systems are those made of silicon, mono or polycrystalline. However, it should be noted that laboratories all over the world, including Poland [1–6], are developing new cell technologies, which is very well illustrated by the chart comparing the *PCE* (Power Conversion Efficiency) of PV cells made in different technologies, developed, updated and available on the website [7] of the *American National Renewable Energy Laboratory* (NREL). Figure 1, in turn, shows a fragment of this graph regarding monocrystalline (blue line) and polycrystalline (green line) silicon cells and heterojunction silicon cells (red line). On the basis of this graph, it should be concluded that currently the highest efficiency is characteristic for heterojunction cells, and is equal to 26.8% [7–9]. Figure 1 shows that over the last twenty years the value of this parameter has been growing fastest in the considered silicon technology for heterojunction cells. In the case of monocrystalline cells, the efficiency is slightly lower and reaches 26.1%. Polycrystalline cells, on the other hand, have the efficiency of 23.3%. It is worth noting that currently commercially available technologies of

Article history: received August 10, 2023; revised September 12, 2023; accepted September 26, 2023; available online February 22, 2024.

silicon cells, for which efficiencies do not exceed 26%, are based on such structures as PERC (*Passivated Emitter and Rear Cell*), PERT (*Passivated Emitter Rear Totally-diffused*), PERL (*Passivated Emitter Rear Locally-diffused*) or TOPCon (Tunnel Oxide-Passivated Contact).

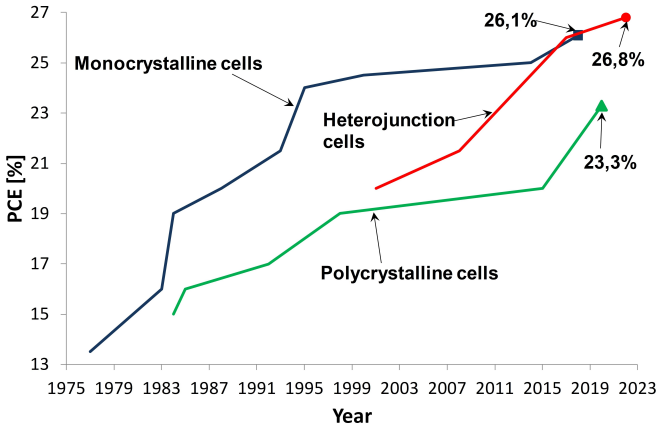

Fig. 1. Efficiency of PV cells based on silicon [7].

Characterization of PV cells usually comes down to providing electrical parameters in STC (*Standard Test Conditions*) and NOCT (*Nominal Operating Cell Temperature*), including, among others, short-circuit current, open-circuit voltage, maximum power, the fill factor, photovoltaic power conversion efficiency, temperature coefficients of changes in selected parameters and operating characteristics presenting the current-voltage relationship for different values of solar irradiance. In addition, in selected cell catalog notes, the influence of temperature on the current-voltage or power-voltage characteristics and the standardized spectral characteristics of the current sensitivity are presented.

In many scientific papers, *e.g.* [5, 10–14, 16, 17], it is postulated that when characterizing photovoltaic cells, it is of great importance to focus on measurements of spectral characteristics presenting the dependence of such parameters as current sensitivity (nomenclature interchangeable with *SR – Spectral Response* or responsivity) and quantum efficiency (in particular, external quantum efficiency *EQE – External Quantum Efficiency*) on the wavelength of optical radiation. Despite the fact that, typically, the spectral characteristics of silicon cells are similar both in terms of quality and quantity, some scientists, *e.g.*, in [14], postulate that during fabrication of PV modules cells are used with not only identical values of electrical parameters, but also having identical spectral characteristics.

The influence of temperature on selected properties of photovoltaic cells is usually determined on the basis of the cell tests conducted at fixed ambient temperatures, *e.g.*, under the *standard test conditions* (STC) the cell temperature is equal to 25°C. In turn, it should be noted that in real conditions the temperature of the working PV cells is different than the ambient temperature, and in particular with high insolation in the summer, it can significantly exceed the ambient temperature. An increase in the temperature of solar cells, described *e.g.*, in [18, 19] is due to, among others, the absorption of thermal radiation and the phenomenon of self-heating resulting from the imperfect conditions of heat dissipation from semiconductor devices [20–22].

As previously mentioned, spectral characteristics are presented in numerous scientific articles, but there are few studies in which the influence of temperature on these characteristics is analyzed. For example, in [10] the characteristics of quantum efficiency of crystal cells made of silicon,

measured in the temperature range from 15°C to 70°C, were presented. According to this work, when increasing temperature, the quantum efficiency slightly increases for the wavelengths above 900 nm. In turn, the paper [11] presents the characteristics of the current sensitivity of cells made of amorphous silicon and CIS cells (cells made of a compound of copper, indium and selenium) obtained in the ambient temperature range from 25°C to 65°C. According to this work, in the case of CIS cells, current sensitivity does not depend on temperature, while in the case of amorphous cells, the value of this parameter for the wavelengths above 600 nm increases when increasing temperature. Therefore, based on selected scientific publications, it can be concluded that values of parameters describing the spectral properties of PV cells change ambiguously when increasing the ambient temperature, and the nature of these changes depends on the type of cell.

In this work, there is presented a measuring system of spectral characteristics of current sensitivity and external quantum efficiency of the silicon solar cells with the obtained results of the measurements of arbitrarily selected commercial crystalline silicon cells. The investigations were carried out at the constant ambient temperature (room temperature equal to 22.5°C), while properly prepared test samples of cells were characterized by the constant temperature value determined by using a heater in the form of a semiconductor diode placed with a given sample on a common heat sink. This paper presents the cell characteristics for the values of temperature: 22.5°C, 51.5°C and 75.5°C. The selected measurement methodology simulates conditions similar to the operating conditions, in which the ambient temperature differs from the temperature of the working PV cells.

2. Tested PV cells

To evaluate spectral properties of silicon photovoltaic cells, two types of cells were arbitrarily selected: a monocrystalline PERC cell marked with the symbol 156.75M4BB from Shenzhen Topsky Energy Co., Ltd. (currently, the next generation of these cells is offered on the market [23]) and a polycrystalline cell marked with the symbol JS156B4 by Yixing JS Solar Co., Ltd. [24]. Both the cells have similar dimensions of 156x156 mm. In Table 1 and Table 2, on the basis of the catalog notes, the values of selected parameters of the tested photovoltaic cells were collected, where: *PCE* - efficiency, P_{MAX} – maximum power, I_{SC} – short-circuit current, U_{OC} – open circuit voltage, I_{MPP} – current at the maximum power point, U_{MPP} – voltage at the maximum power point, *FF* – fill factor, α – temperature coefficient of short-circuit current changes, β – temperature coefficient of open-circuit voltage changes, γ – temperature coefficient of the maximum power changes.

Table 1. Values of selected electrical parameters of the tested PV cells.

Cell symbol	***PCE*** **[%]**	P_{MAX} **[W]**	I_{SC} **[A]**	U_{OC} **[mV]**	I_{MPP} **[A]**	U_{MPP} **[mV]**	***FF*** **[%]**
156.75M4BB	20.4÷21	4.98÷5.13	9.59÷9.75	658÷666	9.11÷9.27	547÷553	72.63÷75
JS156B4	17.2÷19	4.23÷4.67	8.67÷8.99	622÷645	8.13÷8.54	521÷547	59÷65.1

Table 2. Values of selected temperature parameters of the tested PV cells.

Cell symbol	α **[%/K]**	β **[%/K]**	γ **[%/K]**
156.75M4BB	0.02	-0.32	-0.43
JS156B4	0.05	–0.33	–0.38

As can be seen in Table 1, PV cells are characterized by technological dispersion of the operating parameters, as the values of the presented parameters fall within specific ranges. The monocrystalline cell has higher values of electrical parameters compared with the polycrystalline cell. In turn, in the case of temperature parameters, the tested cells are characterized by positive temperature coefficients of changes in the short-circuit current and negative temperature coefficients of changes in the open-circuit voltage and the maximum power, which is typical for the cells of the considered class. As can be seen in Table 2, the values of individual parameters are close to each other.

3. Measuring system of spectral characteristics

Figure 2 presents a diagram of the measuring system used for the investigations. This system was used also in a narrower scope of the research, *e.g.*, in [25, 26]. The source of optical radiation in the considered measuring set is a TLS (*Tunable Light System*) device by Newport [27]. The radiation-emitting element is a broadband xenon lamp with an average electrical power of 300 W. In the TLS device, the signal from the lamp is fed to a monochromator, in whose optical output the desired wavelength of optical radiation is obtained.

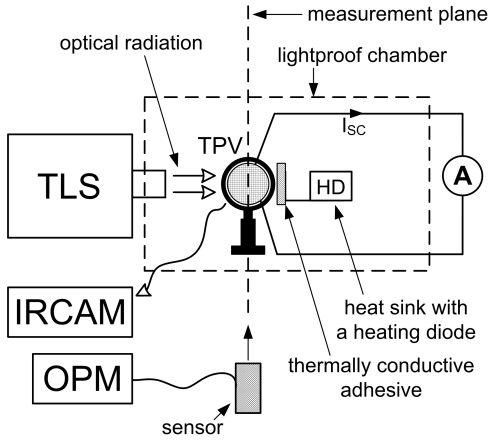

Fig. 2. Measuring system for the investigations of spectral characteristics.

The optical signal stimulates the TPV (*tested photovoltaic cell*), but it is important for this signal to have a constant value of optical power regardless of the wavelengths. For this purpose, TLS calibration is necessary, consisting in measuring the optical power with an OPM (*optical power meter*) in the measurement plane, in which the TPV is installed and fixing the electric power of the lamp for specific wavelengths in such a way that optical radiation is characterized by the same value of optical power for different wavelengths. For the calibration, an OPHIR VEGA optical power meter with a PD300-UV detector was used [28]. In the considered case, for the available spectrum of radiation, the optical power was equal to 180 µW. As a result of optical excitation, short-circuit current I_{SC} flows through the short-circuited terminals of the solar cell. In order to obtain different temperature values of the tested PV cell, the cell was thermally stimulated with a heating diode installed on a heat sink glued to the cell with thermally conductive glue – marked as HD (*heating diode*) in Fig. 2. Determining the proper operating point of the diode enables obtaining the desired temperature of the tested PV cell. Temperature measurement in the system from Fig. 2 was carried out using an IRCAM (*infrared camera*), *i.e.*, a thermal imaging camera.

It should be noted that the diameter of the beam emitted by the TLS is 20 mm. Therefore, the preparation of the test samples consisted in cutting samples from factory-made cells into the shape of a circle with a diameter matching the diameter of the optical excitation beam. The cutting process was carried out using a Trotec fiber laser (emission of radiation with a wavelength of 1064 nm), described in [29].

Then, the cut samples were subjected to a multi-stage process of grinding their edges using P2500 grit sandpaper in order to remove the residues of laser ablation products. Figure 3 shows photos taken with a Keyence VHX-7000 microscope with a ZS200 lens and optical magnification x500, showing the edge of the cell in the area of the metal electrode after the cutting process – Fig. 3a, the edge of the cell in the area of the radiation-absorbing surface after the cutting process – Fig. 3b and the edge of the cell in the area of the metal electrode after the grinding process – Fig. 3c. As it is visible, grinding enables removing the products of laser processing, including melting of semiconductor layers. The effectiveness of the grinding process was assessed by measuring the open-circuit voltage of the prepared samples for constant optical excitation emitted by the halogen lamp. As soon as a constant value of this voltage was observed, without measurable increases in the value after individual grinding stages, the processing of the edge of a given sample was considered complete.

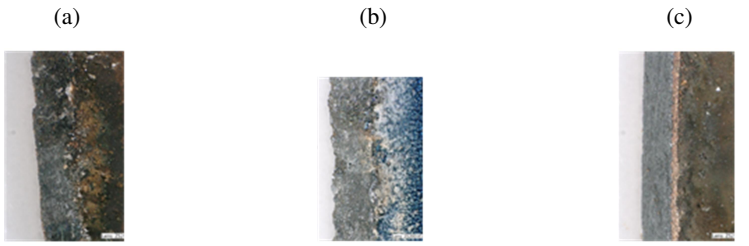

Fig. 3. Edge of the solar cell in the area of metallization (a), edge of the solar cell outside this area before the grinding process (b), edge of the cell in the area of metallization after the grinding process (c).

In order to ensure the purity of the surface absorbing optical radiation, the cell surfaces were cleaned with compressed air. Figure 4a shows the surface of the measured sample after the process of its production – the imaging was performed with the Keyence VHX-7000 microscope with an E500 lens and optical magnification x1000. Figure 4b shows one of the test samples.

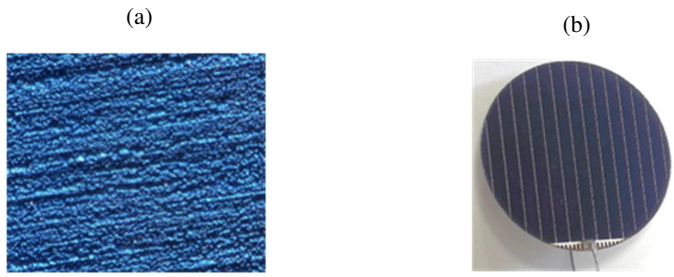

Fig. 4. PV cell surface 156.75M4BB (a), PV cell test sample (b).

Figure 5a shows a photo illustrating the connection of a heating diode with a PV cell. In turn, Fig. 5b shows an example thermogram of the tested PV cell. As can be seen in the figure, the entire area of the PV cell is characterized by the same temperature value. The temperature of the tested cell was measured before the actual measurement process, during which the cell was in the lightproof chamber.

(a) (b)

Fig. 5. Installation of a PV cell and a heating diode on a common heat sink (a), temperature distribution on the surface of the tested PV cell (b).

In the presented measurement system, the spectral current sensitivity (the spectral response) of the photovoltaic cell at the fixed value of I_{SC} current was determined from the relationship:

$$SR(\lambda) = I_{SC}(\lambda)/P_{OPT}(\lambda), \tag{1}$$

where I_{SC} is the short-circuit current of the PV cell for the selected wavelength λ, while P_{OPT} is the optical power stimulating the cell at this wavelength.

In turn, the external quantum efficiency was determined from the formula:

$$EQE(\lambda) = (SR(\lambda) \cdot h \cdot c)/(q \cdot \lambda), \tag{2}$$

where h is the Planck's constant, c is the speed of light in a vacuum, and q is the charge of the electron.

4. Research results

It should be noted that a significant problem associated with spectral measurements using a xenon gas discharge lamp are its characteristic spectral lines. Figure 6 shows the emissivity characteristic of the xenon lamp used (pink line). As you can see, compared with the characteristic of the halogen lamp (blue line), especially in the near infrared range, the xenon discharge lamp is characterized by strong spectral lines.

The TLS calibration performed for spectral lines with a high value of the optical power required the determination of a low value of electric power of the xenon lamp (of the order of tens of watts), which is associated with a low current supplying the lamp, and as a result, its unstable operation and fluctuations of the optical power of the output signal. Hence, ripples appear on the measured spectral characteristics in the near infrared range.

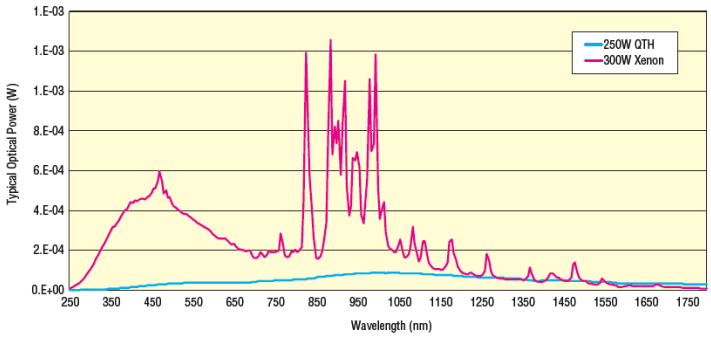

Fig. 6. Spectral characteristic of a xenon lamp [27].

In order to evaluate the usefulness of the measurement system presented in Fig. 2, the measured characteristic of the spectral response of the JS156B4 cell (points) were compared in Fig. 7 with the catalog characteristic (line). As can be seen, a very good agreement of the characteristics was obtained, both in terms of quality and quantity.

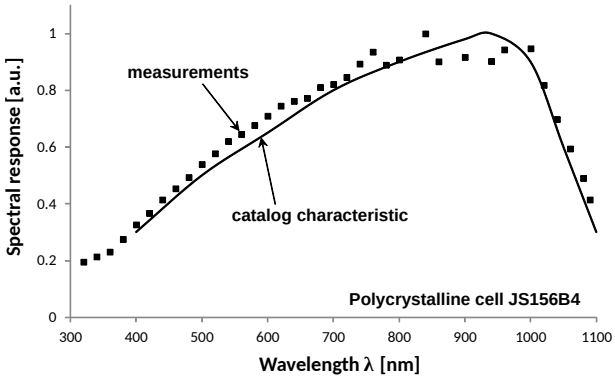

Fig. 7. Comparison of characteristics of spectral response of the JS156B4 cell.

The next four figures show the results of the investigations considering the work of PV cells obtained for three temperature values of these cells: 22.5°C, 51.5°C and 75.5°C. In order to facilitate the analysis and evaluation of the research results, in the figures, apart from the measurement results – points, the characteristics approximated by the fifth-order polynomial represented by solid lines were also plotted.

Figure 8 presents the measured characteristics $SR = (\lambda)$ of the 156.75M4BB cell. As shown in the figure, with an increase of the wavelength, the value of the spectral response of the PV cell increases, assuming for the temperature of 22.5°C the maximum value for the optical wave equal to about 970 nm. An increase in the cell temperature causes a decrease in responsivity in almost the entire examined range of the optical radiation spectrum, and for optical waves with the lengths longer than 1000 nm the points of intersection of these characteristics are also noticeable. After exceeding these points, a higher value of the parameter under consideration is obtained by the cell with a higher temperature. The maximum of the responsivity when increasing temperature shifts

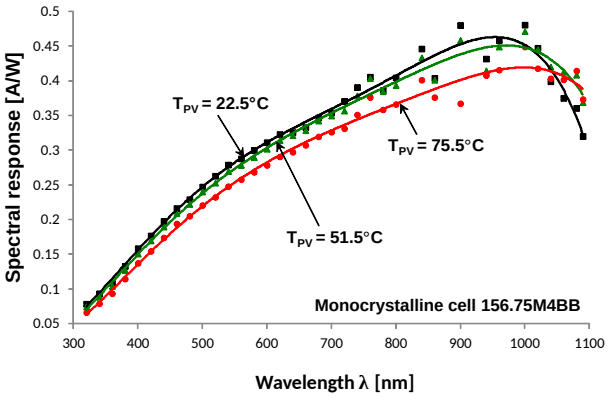

Fig. 8. Characteristics of spectral response of the 156.75M4BB cell.

in the long-wave direction, where for the temperature of 75.5°C it occurs at a wavelength of about 1020 nm. This nature of changes in the responsivity is probably related to the decrease in the value of the silicon bandgap energy as the temperature increases. In the case of the characteristics $SR = f(\lambda)$ of the polycrystalline cell (Fig. 9), it should be noted that it has a slightly lower spectral response compared with the monocrystalline cell, not exceeding the maximum value of 0.45 A/W. The points of intersection of the characteristics occur for the optical wavelengths longer than 950 nm.

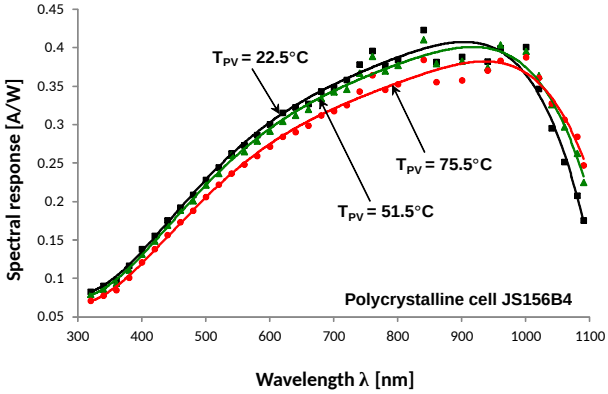

Fig. 9. Characteristics of spectral response of the JS156B4 cell.

Figures 10 and 11 present the $EQE = f(\lambda)$ characteristics of the 156.75M4BB and JS156B4 cells, respectively. As can be seen, the nature of changes in the quantum efficiency in the wavelength domain is completely different than in the current sensitivity domain. For both the tested cells, the *EQE* value increases monotonically, in the case of a monocrystalline cell to a wavelength of about 550 nm, and for a polycrystalline cell to a wavelength of about 630 nm, followed by a slight decrease of the considered value for higher wavelengths. At a wavelength of about 1000 nm – for the JS156B4 cell and 1050 nm – for the 156.75M4BB cell, there is a strong decrease in the quantum efficiency. The higher cell temperature results in a lower value of the quantum efficiency, with a higher value of the quantum efficiency at the intersection points of the higher temperature cell.

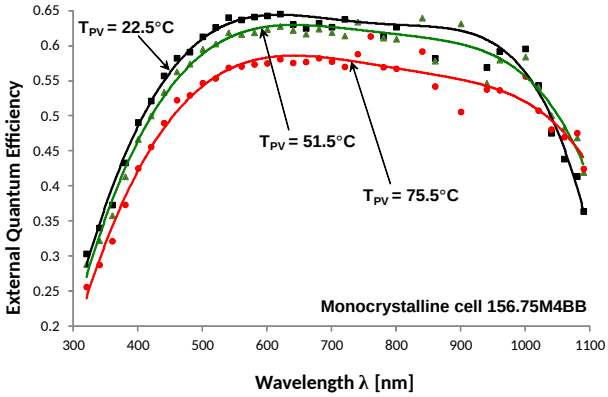

Fig. 10. External quantum efficiency characteristics of the 156.75M4BB cell.

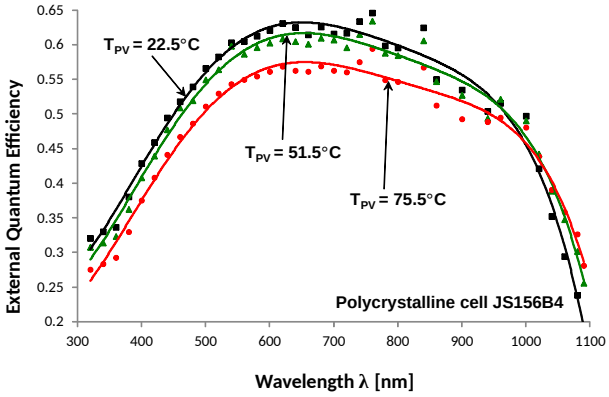

Fig. 11. External quantum efficiency characteristics of the JS156B4 cell.

5. Conclusions

As part of the work, experimental evaluation of spectral properties of two commercial silicon photovoltaic cells was carried out by examining the dependence of the current sensitivity (*SR*) and the external quantum efficiency (*EQE*) on the optical wavelength. For this purpose, the measurement methodology was developed along with the measurement system and the procedure for preparing samples of the investigated solar cells. Two types of cells were arbitrarily selected for the investigations: monocrystalline and polycrystalline. The research tests were carried out at the ambient temperature of 22.5°C for three different temperature values of the tested cells, obtained using an additional heating element. On the basis of the conducted research, it should be concluded that changes in both *SR* and *EQE* when increasing the temperature of PV cells operating at the constant ambient temperature are not unequivocal. In the range of UV and VIS radiation, the values of these quantities decrease when increasing the cell temperature, while in the near infrared range, the cell assumes higher values of these quantities for its higher temperature. The maximum values of the responsivity of the tested silicon cells in a wide range of temperature changes from about 22°C to 75°C are in the range of about 0.45 A/W to 0.35 A/W, respectively. For the optical wavelength of about 1000 nm, there is a rapid decrease in the value of *SR* of the tested cells. In turn, *EQE* of the tested cells in the wavelength range from about 550 nm to about 1000 nm ranges from about 0.5 to about 0.65. Outside the given wavelength range of optical radiation, the value of this parameter strongly decreases.

Acknowledgements

The authors would like to thank Mr. Dawid Chojnowski, a representative of Keyence in Poland, for providing us with the VHX-7000 microscope for investigations.

The research material described in the article was presented at the XXII National Conference on Electronics, Darłowo, Poland, June 11–15, 2023 (the website of the conference: https://kke.umg.edu.pl/).

References

[1] Iwan, A., Bogdanowicz, K., & Przybył, W. (2022). Organiczna warstwa transportująca ładunki dodatnie w polimerowych i perowskitowych ogniwach słonecznych – wybrane aspekty materiałowe i techniczne. *Przegląd Elektrotechniczny*, *98*(9), 178–181, (in Polish). https://doi.org/10.15199/48.2022.09.40

[2] Czapka, T., Woś, A., & Palewicz M. (2018). Wpływ niskotemperaturowej plazmy na właściwości cienkich folii stosowanych do zabezpieczania ogniw fotowoltaicznych. *Przegląd Elektrotechniczny*, *94*(10), 216–220, (in Polish). https://doi.org/10.15199/48.2018.10.50

[3] Szindler, M., & Szindler, M. (2018). Barwnikowe ogniwa fotowoltaiczne z polielektrolitem. Przegląd Elektrotechniczny, 94(8), 32–34, (in Polish). https://doi.org/10.15199/48.2018.08.09

[4] Skolik, M., & Karasiński P. (2017). Jedno- i dwuwarstwowe struktury antyrefleksyjne wytwarzane metodą zol-żel do zastosowań w fotoogniwach krzemowych. Przegląd Elektrotechniczny, *93*(8), 73–76, (in Polish). https://doi.org/10.15199/48.2017.08.19

[5] Szindler, M., Szindler, M., Orwat, J., & Kulesza-Matlak G. (2022). The Al_2O_3/TiO_2 double antireflection coating deposited by ALD method. *Opto-Electronics Review*, *30*(3), 1–6. https://doi.org/10.24425/opelre.2022.141952

[6] Korzec, M., Kotowicz, S., Pająk, A.K, & Schab-Balcerzak, E. (2021). Symmetrical and asymmetrical imino-naphthalimides in perovskite solar cells. *Opto-Electronics Review*, *29*, 175–180. https://doi.org/10.24425/opelre.2021.139755

[7] NREL. *Best Research-Cell Efficiency Chart*. Retrieved August 10, 2023, from https://www.nrel.gov/pv/cell-efficiency.html

[8] Pv magazine. *Longi claims world's highest efficiency for silicon solar cells*. Retrieved August 10, 2023, from https://www.pv-magazine.com/2022/11/21/longi-claims-worlds-highest-silicon-solar-cell-efficiency/

[9] Laboratorium Fotowoltaniczne IMIM PAN. (2022). *Nowy rekord sprawności krzemowego ogniwa słonecznego*. Retrieved August 10, 2023, from https://pvinnowacje.pl/41-aktualnosci/773-nowy-rekord-sprawnosci-krzemowego-ogniwa-slonecznego

[10] Osterwald, C.R., Campanelli, M., Moriarty, T., Emery, K.A., & Williams, R. (2015). Temperature-dependent spectral mismatch corrections. *IEEE Journal of Photovoltaics*, *5*(6), 1692–1697. https://doi.org/10.1109/JPHOTOV.2015.2459914

[11] Müllejans, H., Wagner, T., Merli, F., Jäger-Waldau, A., & Dunlop, E.D. (2004). Changes in spectra response with temperature and irradiance intensity. *Thin Solid Films, 451–452*, 145–151. https://doi.org/10.1016/j.tsf.2003.11.006

[12] Reich, N. H., van Sark, W. G. H. J. M., Alsema, E. A., Kan, S. Y., Silvester, S., van der Heide, A. S. H., Lof, R. W., & Schropp, R. E. I. (2005, June). Weak light performance and spectral response of different solar cell types. *Proceedings of the 20th European Photovoltaic Solar Energy Conference* (pp. 2120–2123).

[13] Lee, S., & Price, K. J. (2017). Spectral responses in quantum efficiency of emerging kesterite thin-film solar cells, *Optoelectronics – Advanced Device Structures*, 341–362, InTech. https://doi.org/10.5772/68058

[14] Talukdar, B., Buragohain, S., Kumar, S., Umakanth, V., Sarmah, N., & Mahapatra, S. (2016). Effect of spectral response of solar cells on the module output when individual cells are shaded. *Solar Energy*, *137*, 303–307. https://doi.org/10.1016/j.solener.2016.08.032

[15] Ananda, W. (2017, July). External quantum efficiency measurement of solar cell. *Proceedings of the 15th International Conference on Quality in Research: International Symposium on Electrical and Computer Engineering*, Indonesia (pp. 450–456). IEEE. https://doi.org/10.1109/QIR.2017.8168528

[16] Zhang, S., Yao, Y., Hu, D., Lian, W., Qian, H., Jie, J., Wei, Q., Ni, Z., Zhang, X., & Xie L. (2019). Application of silicon oxide on high efficiency monocrystalline silicon PERC solar cells. *Energies*, *12*(6). https://doi.org/10.3390/en12061168

[17] Cao, Y., Zhu, P., Li, D., Zeng, X., & Shan, D. (2020). Size-dependent and enhanced photovoltaic performance of solar cells based on Si quantum dots. *Energies*, *13*(18). https://doi.org/10.3390/en13184845

[18] Górecki, K., Dąbrowski, J., Krac, E., & Zarębski, J. (2017). Modelling the influence of weather conditions on properties of the photovoltaic installation. *Proceedings of the 24th International Conference Mixed Design of Integrated Circuits and Systems* (pp. 366–371). IEEE. https://doi.org/10.23919/MIXDES.2017.8005233

[19] Dąbrowski, J., Krac, E., & Górecki, K. (2018). New model of solar cells for SPICE. *Proceedings of the 25th International Conference Mixed Design of Integrated Circuits and Systems* (pp. 338–342). https://doi.org/10.23919/MIXDES.2018.8436819

[20] Zarębski, J., & Górecki, K. (2008). A method of the thermal resistance measurements of semiconductor devices with p-n junction. *Measurement*, *41*(3), 259–265. https://doi.org/10.1016/j.measurement.2006.11.009

[21] Bisewski, D., Myśliwiec, M., Górecki, K., Kisiel, R., & Zarębski, J. (2016). Examinations of selected thermal properties of packages of SiC Schottky diodes. *Metrology and Measurement Systems*, *23*(3), 451–459. https://doi.org/10.1515/mms-2016-0033

[22] Górecki, K., & Górecki, P. (2015) The analysis of accuracy of selected methods of measuring the thermal resistance of IGBTs. *Metrology and Measurement Systems*, *22*(3), 455–464. https://doi.org/10.1515/mms-2015-0036

[23] Topsky Energy Co., Ltd. http://www.topskyenergy.com/Product.html

[24] JS Solar. *JS156B4*. https://www.jssolar.com/81/94.html

[25] Górecki, K., & Dąbrowski, J. (2019, April). Modelling properties of solar cells irradiated from different lighting sources. *Proceedings of the 13th International Conference on Compatibility, Power Electronics and Power Engineering* (pp. 1–5). IEEE. https://doi.org/10.1109/CPE.2019.8862389

[26] Górecki, K., Dąbrowski, J., & Krac, E. (2021). Modeling solar cells operating at waste light. *Energies*, *14*(10). https://doi.org/10.3390/en14102871

[27] Newport Corporation. *DS-TLS Series Tunable Xe Arc Lamp Sources* [Datasheet]. https://www.newport.com/p/TLS-300XR

[28] Ophir Optronics Solutions Ltd. https://www.ophiropt.com

[29] Dąbrowski, J. (2019). Techniki szybkiego wytwarzania prototypowych obwodów drukowanych. *Przegląd Elektrotechniczny*, *95*(9), 165–168, (in Polish). https://doi.org/10.15199/48.2019.09.35

Jacek Dąbrowski graduated from Gdynia Maritime University, Poland, and received the M.Sc. degree in radio-electronics in 2003. In 2007 he received the Ph.D. degree in electronics from the Łódź University of Technology of, Poland. At present, he works in the Department of Marine Electronics at Gdynia Maritime University. His current research activities include measurements and modelling of semiconductor devices and electronic and optoelectronic circuits, especially solar cells and photovoltaic circuits and systems.

Łukasz Buchert received the M.Sc. degree in 2017 from Gdynia Maritime University. Presently, he works at this university as a technician in the Department of Marine Electronics. He deals with measurements in electronics, especially in the field of photovoltaics.

Janusz Zarębski received the M.Sc. and Ph.D. degrees in electronics from the Gdańsk University of Technology, Poland, in 1978 and 1986, respectively, and the D.Sc. degree from the Institute of the Electron Technology, Warsaw, Poland, in 1997. Since 2008 he has been a full professor. Currently, he is Head of the Department of Marine Electronics, Gdynia Maritime University, Poland. His research interest focuses on modelling, analysis and measurements of semiconductor power devices and power electronic circuits, particularly those including electro-thermal effects.